Targeting mitochondrial dysfunction can restore antiviral activity of exhausted HBV-specific CD8 T cells in chronic hepatitis B

Targeting mitochondrial dysfunction in exhausted HBV-specific CD8 T-cells can restore antiviral activity in chronic hepatitis B

Paola Fisicaro[1], Valeria Barili[1], Barbara Montanini[2], Greta Acerbi[1], Manuela Ferracin[3], Francesca Guerrieri[4], Debora Salerno[4], Carolina Boni[1], Marco Massari[5], M. Cristina Cavallo[1], Glenda Grossi[6], Tiziana Giuberti[1], Pietro Lampertico[6], Gabriele Missale[1], Massimo Levrero[4,7,8], Simone Ottonello[2,9] and Carlo Ferrari[1*]

1. Laboratory of Viral Immunopathology, Unit of Infectious Diseases and Hepatology, Azienda Ospedaliero-Universitaria of Parma, Parma, Italy
2. Biochemistry and Molecular Biology Unit, Laboratory of Functional Genomics and Protein Engineering, Department of Life Sciences, University of Parma, Parma, Italy
3. Department of Experimental, Diagnostic and Specialty Medicine – DIMES, University of Bologna, Bologna, Italy
4. Center for Life Nanoscience Laboratory IIT – CNLS, Sapienza University Rome, Italy
5. Unit of Infectious Diseases, IRCCS-Azienda Ospedaliera S. Maria Nuova, Reggio Emilia, Italy
6. 1st Division of Gastroenterology, Fondazione IRCCS Ca' Granda, Ospedale Maggiore Policlinico, Università degli Studi di Milano
7. Department of Internal Medicine (DMISM), Sapienza University Rome, Italy
8. Cancer Research Center of Lyon (CRCL) - INSERM U1052, Lyon, France
9. Biopharmanet-Tec Laboratory, University of Parma, Parma, Italy

***Corresponding author**: Prof. Carlo Ferrari MD, Laboratory of Viral Immunopathology, Unit of Infectious Diseases and Hepatology, Azienda Ospedaliero-Universitaria of Parma, Via Gramsci, 14, 43126 Parma, Italy.

e-mail: cferrari00@gmail.com

Phone: +39-0521-703622; Fax: +39-0521-703857

ABSTRACT

HBV-specific CD8-T cells are functionally exhausted in chronic hepatitis B infection and this condition can only be partially corrected by modulation of inhibitory pathways, suggesting that a more complex molecular interplay underlies T-cell exhaustion. To gain a broader insight into this process and identify additional targets for restoring T cell function, we compared the transcriptome profiles of HBV-specific CD8-T cells from acute and chronic patients with those of HBV- and FLU-specific CD8-T cells from patients able to resolve HBV infection spontaneously and from healthy subjects. The results indicate that exhausted HBV-specific CD8-T cells are markedly impaired at multiple levels and show substantial down-regulation of various cellular processes centered on extensive mitochondrial alterations. A significant improvement of mitochondrial and antiviral CD8 functions was elicited by mitochondrion-targeted antioxidants, suggesting a central role for reactive oxygen species (ROS) in T cell exhaustion. Thus, mitochondria represent promising targets for novel reconstitution therapies in chronic hepatitis B infection.

Treatment of chronic hepatitis B (CHB) currently relies on either short-term IFNα therapy or long-term administration of nucleos(t)ide analogues (NUC)[1]. Frequent side-effects and a limited rate of sustained antiviral responses are the main drawbacks of IFN therapy, whose ultimate goal is primarily to convert an active into an inactive infection, rather than to completely suppress virus replication. NUCs are very effective at inhibiting HBV replication, but because of the risk of HBV reactivation they can only be withdrawn after anti-HBs antibodies become detectable. Since HBsAg declines very slowly during NUC therapy and detection of anti-HBs antibodies is a rare and late event, life-long NUC administration is frequently required. There is thus an urgent clinical need to define novel therapeutic strategies for HBV infection. These strategies should be well tolerated, short-term, and capable of inducing durable HBV control alone, or in combination with other available drugs by either consolidating the effect of IFNα or by speeding-up HBsAg clearance in NUC-treated patients.

In chronic hepatitis B patients, antiviral immune responses are severely depressed[2,3] and reconstitution of effective antiviral immune control is considered a rational new avenue to cure infection. Hyperactivation of negative regulatory pathways centered on co-inhibitory molecules such as PD-1[4,5], but also involving suppressive cytokines, inhibitory Treg cells and prostaglandin receptors has been reported in various models of chronic virus infection[6-9]. The potential relevance of these suppressive mechanisms has also been investigated in HBV infection and *in vitro* modulation of inhibitory pathways has been shown to promote reconstitution of HBV-specific T-cell function[10-15]. However, these targeted "monovalent" strategies are only effective in a fraction of chronic HBV patients and functional recovery in responding subjects is always partial.

In order to devise more effective immune reconstitution strategies, additional molecular targets must be identified and a systematic analysis of the genes and pathways that are misregulated in exhausted T cells from naturally infected patients represents an essential first step in this direction. With this goal in mind, we performed a genome-wide expression profiling of exhausted HBV-specific CD8 T-cells from chronic patients, which revealed an extensively downregulated gene expression program compared to functionally competent CD8 T-cells from patients who spontaneously resolved infection. This impairment was consistent with a severe energetic, metabolic and genome integrity defense impairment which was the hallmark of exhausted CD8 T-cells and a marked recovery of antiviral T-cell capacity was achieved by

treating cells with mitochondria-targeted antioxidant compounds. These results identify mitochondrial dysfunction as a promising target for novel combined reconstitution therapies in CHB.

RESULTS

Genome-wide expression profiling of HBV-specific CD8 T-cells from acute and chronic HBV patients. We used oligo-60-mer whole genome microarrays to profile the transcriptomes of dextramer-stained HBV-specific CD8 T-cells sorted from the peripheral blood of patients in the acute (5) and chronic (4) phase of hepatitis B (**Fig. 1a**). CD8 T-cells from 4 patients who spontaneously resolved infection and influenza (FLU)-specific CD8 T-cells from 5 healthy subjects served as controls. On a total of 18,631 genes with above background expression levels, we identified a subset of 504 genes that were differentially expressed in acute, resolved and chronic patients by ANOVA (**Fig. 1b, Supplementary Table 1**). Principal-component-analysis of ANOVA-filtered data showed a clear segregation of the three patient groups (**Fig. 1c**). By a post-hoc SNK test, 382, 286 and 479 genes emerged as differentially expressed from the comparison of acute *vs.* resolved, chronic *vs.* resolved, and acute *vs.* chronic patients, respectively. The overlap between the differentially expressed genes retrieved from individual comparisons is illustrated in **Fig. 1d**.

Analysis of the 504 differentially expressed genes with the unsupervised Self-Organizing-Maps algorithm[16] identified six clusters of genes displaying distinct (but internally consistent) expression profiles in "acute" or "chronic" vs "resolved" patients (**Supplementary Fig. 1**).

We then applied pathway enrichment analysis to gain insight into the cellular functions of the genes displaying distinct expression profiles in the acute and chronic stages of infection (**Supplementary Fig. 1, Supplementary Table 2**). In keeping with the notion that acute viral infections induce a sustained proliferation of virus-specific CD8 T-cells[17], genes involved in cell cycle regulation and DNA repair were found among the most up-regulated, acute stage-preferential genes in cluster #0. The gene coding for transcription factor E2F2, which positively regulates DNA replication and the G1/S phase transition, was also present in this cluster and was up-regulated by 15-fold. Mitochondrion-related processes such as fatty acid oxidation and heme biosynthesis were also highly represented among the acute stage-upregulated genes, along with genes coding for proteins involved in T-cell activation and inflammation, including several components of the PI3K and IL-1 signaling pathways. Among the transcripts down-regulated in the acute phase (cluster #5), we found multiple ribosomal and ribosomal-like

protein mRNAs, four lncRNAs and the mRNAs of four zinc-finger proteins of unknown function.

Consistent with a general T-cell activation in the acute phase and a functionally depressed T-cell condition in the chronic phase of infection[18], many genes displayed an opposite expression trend in relation to the phase of infection (cluster #1), including genes coding for proteins involved in PI3K signaling, cytoskeleton regulation and vesicle-mediated transport (**Supplementary Fig. 1**, **Supplementary Table 2**). Another highly enriched pathway, up-regulated in acute patients and down-regulated in chronic patients, bears upon mitochondrial function, including oxidative phosphorylation and electron transport genes. Additional genes strongly down-regulated in exhausted CD8 T-cells are related to proteasome/lysosome function (cluster #1) and to general cell metabolism, including vitamin/cofactor biosynthesis, RNA transport and translation (cluster #2) (**Supplementary Fig. 1**).

Combined analysis of clusters #3 and #4, which are comprised of genes up-regulated in chronic patients, revealed a number of negative transcriptional regulators with DNA-binding C2H2-zinc finger and repressive Krüppel-associated box domains (**Supplementary Fig. 1**, **Supplementary Table 2**). Also consistent with an exhausted T-cell function is the up-regulation of Hedgehog signaling components (PTCH1, HHIP) and of members of the 70 kDa heat-shock protein family (HSPA1L), which have been reported to be involved in the modulation of T-cell function[19-21]. Additional up-regulated transcripts in these clusters (*CBS* and *SARDH*) are related to amino acid (cysteine and glycine) metabolism.

Global downregulation of mitochondrial function and other core cellular processes in HBV-specific CD8 T-cells from chronic patients. We then used Gene-Set Enrichment Analysis (GSEA)[22] to further investigate the processes underlying T-cell exhaustion in chronic HBV infection. We initially focused on the comparison between chronic and resolved patients, and interrogated the entire dataset against the Molecular Signatures Database. As shown in **Fig. 2a**, which reports gene-sets with a False Discovery Rate <0.1 (see **Supplementary Table 3** for a complete list of misregulated genes), all relevant pathways identified by GSEA are down-regulated in chronic patients and most of them overlap with the pathways revealed by ANOVA. In particular, GSEA confirmed mitochondrial dysfunction as a major abnormality in CD8 T-cells from chronic patients (**Fig. 2a**,**b**). It also extended the list of potential respiratory defects

to multiple, functionally interrelated levels (**Fig. 2c**), including core mitochondrial (mt) processes such as electron transport, mt-protein synthesis, transport across mitochondrial membranes and metabolism. Genes coding for electron transport chain components, including many subunits of complex I (NADH dehydrogenase), II (succinate dehydrogenase), III (cytochrome c reductase), IV (cytochrome c oxidase) and V (ATP synthase); components of the machinery responsible for transcription/translation of the 13 OXPHOS proteins encoded by the mt-genome, such as the mitochondrial RNA polymerase POLRMT and the mt-transcription factor TFAM but also mitochondrial translation and mt-tRNA maturation components; genes related to cellular metabolism, particularly fatty acid and amino acid metabolism, the biosynthesis of heme and other Fe^{2+}-containing cofactors; and the mitochondrial quality-control system, including the morphogenetic mt-regulator and cristae stabilizer OPA-1, were among the genes that are down-regulated in exhausted T-cells (**Fig. 3a** and **Supplementary Table 3**).

Genes encoding 26S proteasome subunits, including the 20S proteolytic core and the 19S and 11S regulatory particles were also found to be markedly down-regulated in chronic infection (**Fig. 2a,b**). The latter are key components of the immune-proteasome and a functional decline of the ubiquitin-proteasome pathway[23] has been associated with the immune response dysfunction that accompanies T-cell aging[24].

Another group of transcripts down-regulated in chronic patients code for proteins involved in DNA repair (**Fig. 2a,b**). These include p53-dependent components, such as the ATM kinase, whose deficiency has been associated with immune senescence[25,26], but also p53-independent DNA repair proteins (RAD 17, 21, 23A, 23B) and the repair DNA polymerase POLH.

A number of mRNAs coding for nuclear RNA polymerase subunits, general transcription factors and chromatin proteins, including core histones, are similarly down-regulated in exhausted CD8 T-cells (**Fig. 2a,b**). Some of the above components (e.g., the telomere protein TERF2IP) play a direct role in genome integrity defense.

Although down-regulation is the prevalent transcriptional phenotype of exhausted T-cells (**Fig. 2a,b**), some genes appear to be up-regulated. As revealed by ANOVA, most of these genes code for negative transcriptional regulators or otherwise repressive components, including multiple C2H2 zinc finger and KRAB domain-containing proteins, and the histone deacetylase HDAC1.

Altogether, these findings indicate a broad functional impairment of exhausted virus-specific CD8 T-cells. This conclusion is corroborated by the concordant results, including the extensive

misregulation of mitochondrial function-related genes, obtained from a parallel transcriptome analysis comparing HBV-specific CD8 T-cells from chronic patients with FLU-specific CD8 T-cells from healthy subjects (**Supplementary Fig. 2),** as well as from the same chronic patients (data not shown).

Molecular and functional validation of the mitochondrial and proteasomal dysfunctions. Because of their multiple roles in cell metabolism as well as in T-cell activation, differentiation and function[27,28,29] (**Fig. 3a**), the mitochondrion and the proteasome were selected as targets for molecular and functional validation of transcriptome data. To this end, the expression levels of the 27 most significantly down-regulated mitochondrion and proteasome-related genes retrieved from ANOVA and GSEA were evaluated by Nanostring technology in sorted HBV-specific CD8 T-cells from three additional chronic patients, using three resolved patients as controls. 74% of the selected genes were confirmed to be down-regulated in the HBV-specific CD8 T-cell population (chronic *vs.* resolved gene expression ratio < 0.8) and 67% of them were also found to be down-regulated in PD-1+/dextramer+ cells from chronic patients, compared to dextramer+ CD8 T-cells from resolved patients (**Fig. 3b**). Notably, the PD1+ fraction sorted from the total CD8 T-cell population showed a completely different gene expression profile, with 83% of the 23 selected mitochondrion-related genes up-regulated (**Fig. 3b**).

To assess whether the dysregulated transcriptional profile is accompanied by a corresponding alteration of protein levels, dextramer+ CD8 T-cells were co-stained with monoclonal antibodies targeting cytochrome c (CyC) and ATP5O, two components of the electron transport chain (ETC). As shown in **Supplementary Fig. 3a**, both ETC proteins are expressed at lower levels in chronic patients compared to resolved and healthy controls.

To functionally validate mitochondrial gene dysregulation, we then used the mitochondrial membrane potential (MMP)-sensitive dyes JC-1 and DiOC6 and the MMP-insensitive dye MitoTracker Green to gain insight into the MMP and the mitochondrial mass of CD8 T-cells from chronic, acute and resolved patients, as well as from healthy subjects. As shown in **Fig. 3c, d** and in **Supplementary Fig. 3b**, following anti-CD3 stimulation, dextramer-positive CD8 T-cells from chronic patients displayed a reduced mitochondrial polarization and mass biogenesis compared to resolved patients and to healthy controls. A similar differential behavior was observed in the PD-1+ subset of HBV-dextramer-positive CD8 T-cells from chronic patients,

thus further supporting the existence of a functional mitochondrial impairment associated with T-cell exhaustion (**Fig. 3c,d**). Finally, we analyzed reactive oxygen species (ROS) levels in virus-specific CD8 T-cells from chronic patients using the mt-superoxide-specific dye MitoSOX Red and compared them with those of CD8 T-cells from resolved and healthy controls. A significantly higher mitochondrial superoxide content was detected in unstimulated cells from chronic patients compared to healthy and resolved controls (**Fig. 3e**). Upon anti-CD3 stimulation, superoxide levels were found to be significantly increased in functional CD8 T-cells from control subjects, whereas a mixed response with the majority of samples exhibiting a decline of superoxide levels was observed in exhausted lymphocytes from chronic patients (**Fig. 3e**).

For proteasomal function testing, we used the ProteoStat aggresome dye, which specifically detects denatured protein cargos associated with aggresomes and aggresome-like inclusion bodies. As shown in **Supplementary Fig. 4,** following anti-CD3 stimulation, a considerably greater content of aggresomes -an indication of a defective aggresome degradation by the ubiquitin-proteasome system- was observed in virus-specific CD8 T-cells from chronic patients compared to resolved patients and healthy controls.

Functional restoration of exhausted HBV-specific CD8 T-cells by treatment with mitochondria-targeted antioxidants. Next, we took advantage of the mitochondria-targeted (MT) antioxidants mitoquinone (MitoQ)[30] and the piperidine-nitroxide MitoTempo[31] to ask if the mitochondrial dysfunction of exhausted CD8 T-cells can be reversed. To this end, PBMCs from chronic patients were stimulated overnight with a mixture of 15-mer HBV peptides in the presence or absence of MT-antioxidants. As shown in **Fig. 4a**, MT-antioxidant treatment markedly reduced the fraction of CD8 T-cells undergoing MMP depolarization upon stimulation with HBV peptides. The same treatment coupled with peptide stimulation, increased superoxide levels in HBV-specific CD8 T-cells from chronic patients, which thereby acquired a behavior similar to that previously observed in anti-CD3 stimulated cells from healthy and resolved controls (**Fig. 4b**). Moreover, we observed a significant increase of the ETC proteins CyC and ATP5O in antioxidant-treated short-term T-cell cultures generated by HBV-specific peptide stimulation of PBMCs from chronic patients compared to untreated cultures (**Fig. 4c**). Under the same conditions, antioxidant treatment also reduced the fraction of

annexin V+ 7AAD+ HBV-specific CD8 T-cells (**Supplementary Fig. 5b,c**), likely as a result of the known pro-apoptotic effect of superoxide species[32].

We then assessed the ability of the MT-antioxidants to improve antiviral function and viability of T-cells. To this end, short-term T-cell lines, generated by HBV-core peptide stimulation of PBMCs from 27 chronic patients, were expanded in the presence or absence of MitoQ and MitoTempo and tested for IFNγ and TNFα production by intracellular cytokine staining. T-cell viability, capacity of expansion and cytokine production were significantly enhanced by MitoQ in stimulated CD8 T-cells (**Supplementary Fig. 5a,b,c**), with mean increases of 3.4- and 2.4-fold for IFNγ and TNFα, respectively (**Fig. 5a)**. An even greater enhancement of cytokine production (5.1- and 3.4-fold, respectively) was induced by MitoTempo (**Fig. 5a**). Collectively, IFNγ and/or TNFα production was increased by more than 1.5 fold in 21 (78%) and 25 (93%) of the 27 tested patients by MitoQ and MitoTempo, respectively, with all but one patient responding to at least one MT-antioxidant. Double-positive, IFNγ/TNFα-producing CD8 T-cells, which have been associated to an enhanced capacity to control viral infection[33], were also significantly increased by MT-antioxidant treatment (**Fig. 5a**). Importantly, IFNγ production was restored to levels comparable to those of CD8 T-cells from "resolved" patients capable of controlling infection. Similar results regarding IFNγ production were obtained with total $CD3^+$ T cells (**Fig. 5b**).

As further shown in **Fig. 5c**, MitoQ also proved to be effective on liver-infiltrating, lesional T-cells and improved cytokine production by intrahepatic CD8 and CD4 T-cells in five out of six tested chronic patients.

The MT-antioxidant effect was significantly more potent on exhausted HBV-specific CD8 T-cells than on functional CD8 T-cells of different virus-specificities. Although a slightly increased cytokine production (mean fold-increases for IFNγ and TNFα: 1.09 and 0.99 with MitoQ; 1.03 and 0.98 with MitoTempo) was also observed in some antioxidant-treated FLU-specific T-cells generated by FLU-peptide stimulation of PBMCs from 9 chronic HBV patients, both antioxidants were more effective on HBV-specific CD8 T-cells (mean fold-increase for IFNγ and TNFα: 8.7 and 14 with MitoQ; 12 and 14.3 with MitoTempo) (**Fig. 6a**). Furthermore, a very weak effect of antioxidant treatment was observed on the whole T-cell population (i.e., anti-CD3-stimulated PBMCs), with no significant increase of either cytokine elicited by MitoTempo and only a slight, non-significant enhancement by MitoQ (**Fig. 6b**). Similarly, only

a modest effect was induced by both MT-antioxidants on HBV-core peptide-stimulated PBMCs from 12 resolved patients, with an enhancement of cytokine production considerably lower than that observed in chronic HBV patients **(Fig. 6c)**.

Altogether these results indicate that MT-antioxidants are effective on exhausted T-cells, but have little effect on functionally competent T-cells.

DISCUSSION

By delineating the dysregulated gene expression networks underlying chronic HBV infection, this study provides novel insights on T-cell exhaustion in a clinically significant setting and identifies a new therapeutic target for a viral disease of major public health relevance. First, the gene expression profile of HBV-specific CD8 T-cells from chronic patients is consistent with a substantial functional impairment at the energetic, metabolic and biosynthetic level that affects multiple core processes ranging from proteasome-dependent protein turnover, to DNA repair, transcription and cytoskeleton dynamics. Second, the predominant feature is a global down-regulation of gene expression that is further amplified by the up-regulation of genes with negative regulatory activity, including co-inhibitory receptors (**Supplementary Fig. 6**). Third, among the various dysregulated processes, mitochondrial function appears to be extensively defective and its restoration by mitochondria-targeted antioxidants elicited functional T-cell reconstitution in the majority of the tested chronic HBV patients, with a strongly preferential effect on HBV-specific T-cells.

The picture of exhausted HBV-specific CD8 T-cells that emerges from our study thus highlights a profound and wide-ranging cellular perturbation centered on mitochondrial dysfunction, which is known to negatively affect T-cell specific activities such as T-cell activation, signaling and effector function[27,28]. This likely compromises multiple energy-requiring processes such as macromolecular biosynthesis, DNA replication and repair, cell motility, vesicle trafficking and membrane transport, ultimately affecting T-cell antiviral effector capacity[34]. In line with this scenario, exhausted CD8 T-cells from chronic patients and actively proliferating CD8 T-cells from acute patients displayed opposite expression trends for genes involved in TCR- and coreceptor-binding dependent signaling pathways. These include different sets of genes strongly down-regulated in chronic and up-regulated in acute patients, such as those involved in class I PI3K/AKT signaling, which is directly linked to CD28 co-stimulation[35], and in actin cytoskeleton dynamics, which is important for T-cell activation and whose alteration may cause TCR signaling defects[36]. A similarly divergent regulation was observed for cytoskeleton-related genes coding for vesicle/lysosomal trafficking components.

Similar defects, including the divergent regulation of genes involved in genome integrity maintenance, have been reported for virus-specific lymphocytes from acutely and chronically

LCMV-infected mice[37,38]. Notably, the GSEA data we obtained from comparison of virus-specific CD8 T-cells from patients in the acute *vs.* the resolution phase of HBV infection are highly concordant with those reported for the comparison of effector and memory CD8 cells in the LCMV mouse model[37,39] (**Supplementary Fig. 7)**.

A significant overlap was also observed between the dysregulated transcriptional profiles of HBV and LCMV exhausted CD8 T-cells[37] (**Supplementary Fig. 7)**, which show similar mitochondrial abnormalities and an enhanced sensitivity to apoptotic death by a subset of exhausted cells[40]. Also relevant are previous observations on the presence of CD8 T-cells with dysfunctional mitochondria in HIV[41] and our preliminary data indicating a similar MMP polarization defect, albeit associated with an overall different gene dysregulation profile, in HCV-specific T-cells from chronic hepatitis C patients (Barili V, Fisicaro P, Ottonello S, Ferrari C, unpublished results). While mitochondrial impairment does not appear to be a unique feature of HBV infection, our data strongly support a key role of such dysfunction in HBV-associated exhaustion. In fact, the same mitochondrial gene dysregulation signature was detected in the PD-1+ subset of the HBV-specific but not of the total CD8 T-cell population, where T-cells of HBV-unrelated specificity, not expected to be exhausted, are predominant.

Most of the processes we found to be dysregulated in exhausted CD8 T-cells are reminiscent of functional defects previously associated with immune cell senescence, which is linked to mitochondrial dysfunction and elevated ROS levels[42]. This is not totally unexpected if one considers that T-lymphocytes are long-lived cells and T-cell senescence can be accelerated under conditions of persistent immune activation such as chronic infections, as well as in the elderly and in some premature immune-aging pathologies[43,44]. For example, a strikingly reduced CD28 expression, as observed in exhausted HBV-specific T-cells (**Supplementary Fig. 6**), is causally associated with T-cell senescence[45]. Genome-safeguard processes[46,47] as well as proteasome and autophagic lysosome-dependent protein turnover[43,48] have also been shown to be deteriorated in senescent cells. Similar considerations hold for the protein machinery that controls mt-genome function and integrity[49,50].

Considering the extensive mitochondrial gene dysregulation occurring in HBV-specific CD8 T-cells from chronic patients and the multifaceted processes associated with mitochondria, which can affect T-cell proliferation and effector function[27,28,34], we reasoned that these organelles may represent a focal point in the functional deterioration of exhausted T-cells. In line with this

hypothesis, we found that treatment with two different MT-antioxidants corrected the MMP depolarization defect and the elevated ROS content of these cells, leading to a significantly improved cellular viability and antiviral activity. Whether MT-antioxidants may be less effective in the low-oxygen environment of the liver[51], where T-cell energy metabolism might predominantly rely on glycolysis[52], remains an open issue, although we observed a positive effect of MitoQ on liver-infiltrating T-cells.

Since only HBV-core peptides were employed to study T-cell reactivity, we cannot exclude that an even greater functional T-cell restoration might be achieved with the use of a larger variety of viral epitopes. Remarkably, MT-antioxidants had only a marginal effect on the overall T-cell population and on functional T-cells. This should reduce the risk of an indiscriminate amplification of T-cell responses and the occurrence of autoimmune reactions under *in vivo* treatment conditions.

Mitochondrial homeostasis and energetic metabolism directly affect T-cell function, and an efficient metabolic reprogramming, which is crucial to dictate T-cell fate, strictly depends on mitochondrial plasticity[27,28,40,52,53]. In fact, T-cell activation has been shown to rely on mitochondrial biogenesis and polarization capacity[54] as well as on a balanced ROS production[27]. Conversely, elevated ROS levels promote T-cell death[32]. Thus, the high ROS levels detected in exhausted T-cells may play a direct role in their dysfunction and MT-antioxidants may well preserve T-cell viability by limiting ROS increase.

Exhausted T-cells also display a marked down-regulation of genes coding for specific mitochondrial proteins, such as CPT-1a, which is involved in T-cell memory generation[55], TFAM, ETC complex I and the mt-fusion protein OPA-1, which are all up-regulated in CD8 memory T-cells[55,56,57]. The inability to switch from glycolysis to oxidative phosphorylation, accompanied by a lowered MMP and an increased mitochondrial size has been reported recently as a prominent defect of exhausted HBV-specific CD8 T-cells[52]. Our results, stemming from an unbiased transcriptome analysis of HBV-specific exhausted CD8 T-cells, followed by an extensive functional validation not involving any cell manipulation and with the systematic use of CD8 T-cells from acute and spontaneously resolving patients as controls, unveiled a mitochondrion-centered but more broadly altered gene expression program.

Mitochondrial gene dysregulation may represent a physiological phenomenon aimed at limiting the pathogenic effects caused by excessive effector responses, which may become detrimental under conditions of persistent T-cell stimulation, as in chronic infections. The extremely low

numbers of virus-specific CD8 T-cells that can be retrieved in the HBV model of chronic infection do not allow, however, to draw any firm conclusion regarding the occurrence and potential role of mitochondrial dysregulation in individual T-cell differentiation subsets.

Given the extensively dysfunctional condition that characterizes HBV-specific CD8 T-cells it is quite unlikely that single-target therapeutic strategies can lead to a full recovery, which would require, instead, a broader approach capable of affecting multiple dysregulated pathways at once. According to this view, it is not too surprising that MT-antioxidant-mediated correction of a central process such as mitochondrial function, proved to be so effective in restoring antiviral T-cell activity and viability. Indeed, CD8 T-cells from virtually all tested HBV chronic patients were responsive to at least one MT-antioxidant, with a recovery of antiviral function comparable to that of CD8 T-cells from patients who spontaneously control infection. Our findings on the T-cell function improvement promoted by MT-antioxidants, together with previous observations regarding the lack of toxicity and the liver protection afforded by MitoQ oral administration in HCV-infected patients not responding to pegylated-interferon plus ribavirin[58], point to the potential of these compounds as new drugs for the functional restoration of exhausted CD8 T-cells in chronic HBV infection.

DATA AVAILABILITY STATEMENT

Microarray expression data are available at NCBI GEO: GSE67801.

ACKNOWLEDGMENTS

We thank Mike Murphy (MRC Mitochondrial Biology Unit Wellcome Trust, Cambridge, UK) for the gift of a MitoQ sample, Silvio Bicciato (Department of Life Sciences, University of Modena and Reggio Emilia, Italy) for introducing us to GSEA, and the Microarray Facility at the University of Ferrara (http://ltta.tecnopoloferrara.it/bioinformatica.php) for help in the initial phase of bioinformatic analysis. We are also grateful to Andrea Cossarizza (Department of Surgery, Medicine, Dentistry and Morphological Sciences, University of Modena and Reggio Emilia, Italy) and Angelo Merli (Department of Life Sciences, University of Parma, Italy) for helpful discussions. This work was supported by a grant from Regione Emilia-Romagna, Italy (Programma di Ricerca Regione-Università 2010-2012; PRUa1RI-2012-006, FC), by a grant (2012.0033, FC) from Fondazione Cassa di Risparmio di Parma (Italy), and by

a FIRB grant (RBAP10TPXK, FC) from the Italian Ministry of Education, University and Research (MIUR, FC).

Author contributions. **PF**: study design, design and execution of the experiments; data acquisition, analysis and interpretation; writing of the manuscript. **VB**: execution of experiments; data acquisition, statistical analysis and interpretation, contribution to manuscript drafting **BM**: microarray data handling, including GSEA and network analysis. **GA:** execution of experiments **MF**: microarray data analysis. **FG, DS:** execution of Nanostring experiments**.** **CB**: analysis of cell-based assays data and patients' characterization. **MM, GG, TG, PL:** recruitment and characterization of patients. **MCC**: technical support with patients' characterization. **GM**, **ML:** critical revision of the manuscript; **SO**: study design, data mining and interpretation, writing and revising the manuscript. **CF**: study concept and supervision, data analysis and interpretation, writing and revising the manuscript, funding retrieval.

COMPETING FINANCIAL INTERESTS

The authors declare no competing financial interests.

REFERENCES

1. European Association For The Study Of The, L. EASL clinical practice guidelines: Management of chronic hepatitis B virus infection. *J Hepatol* **57**, 167-85 (2012).
2. Bertoletti, A. & Ferrari, C. Innate and adaptive immune responses in chronic hepatitis B virus infections: towards restoration of immune control of viral infection. *Gut* **61**, 1754-64 (2012).
3. Rehermann, B. & Nascimbeni, M. Immunology of hepatitis B virus and hepatitis C virus infection. *Nat Rev Immunol* **5**, 215-29 (2005).
4. Barber, D.L. et al. Restoring function in exhausted CD8 T cells during chronic viral infection. *Nature* **439**, 682-7 (2006).
5. Odorizzi, P.M. & Wherry, E.J. Inhibitory receptors on lymphocytes: insights from infections. *J Immunol* **188**, 2957-65 (2012).
6. Alatrakchi, N. & Koziel, M. Regulatory T cells and viral liver disease. *J Viral Hepat* **16**, 223-9 (2009).
7. Chen, J.H. et al. Prostaglandin E2 and programmed cell death 1 signaling coordinately impair CTL function and survival during chronic viral infection. *Nat Med* **21**, 327-34 (2015).
8. Ng, C.T. & Oldstone, M.B. IL-10: achieving balance during persistent viral infection. *Curr Top Microbiol Immunol* **380**, 129-44 (2014).
9. Veiga-Parga, T., Sehrawat, S. & Rouse, B.T. Role of regulatory T cells during virus infection. *Immunol Rev* **255**, 182-96 (2013).
10. Bengsch, B., Martin, B. & Thimme, R. Restoration of HBV-specific CD8+ T cell function by PD-1 blockade in inactive carrier patients is linked to T cell differentiation. *J Hepatol* **61**, 1212-9 (2014).
11. Boni, C. et al. Characterization of hepatitis B virus (HBV)-specific T-cell dysfunction in chronic HBV infection. *J Virol* **81**, 4215-25 (2007).
12. Fisicaro, P. et al. Combined blockade of programmed death-1 and activation of CD137 increase responses of human liver T cells against HBV, but not HCV. *Gastroenterology* **143**, 1576-1585 e4 (2012).
13. Nebbia, G. et al. Upregulation of the Tim-3/galectin-9 pathway of T cell exhaustion in chronic hepatitis B virus infection. *PLoS One* **7**, e47648 (2012).
14. Raziorrouh, B. et al. The immunoregulatory role of CD244 in chronic hepatitis B infection and its inhibitory potential on virus-specific CD8+ T-cell function. *Hepatology* **52**, 1934-47 (2010).
15. Schurich, A. et al. Role of the coinhibitory receptor cytotoxic T lymphocyte antigen-4 on apoptosis-Prone CD8 T cells in persistent hepatitis B virus infection. *Hepatology* **53**, 1494-503 (2011).
16. Tamayo, P. et al. Interpreting patterns of gene expression with self-organizing maps: methods and application to hematopoietic differentiation. *Proc Natl Acad Sci U S A* **96**, 2907-12 (1999).
17. Latner, D.R., Kaech, S.M. & Ahmed, R. Enhanced expression of cell cycle regulatory genes in virus-specific memory CD8+ T cells. *J Virol* **78**, 10953-9 (2004).
18. Wherry, E.J. & Ahmed, R. Memory CD8 T-cell differentiation during viral infection. *J Virol* **78**, 5535-45 (2004).
19. Pockley, A.G., Muthana, M. & Calderwood, S.K. The dual immunoregulatory roles of stress proteins. *Trends Biochem Sci* **33**, 71-9 (2008).
20. Rowbotham, N.J., Hager-Theodorides, A.L., Furmanski, A.L. & Crompton, T. A novel role for Hedgehog in T-cell receptor signaling: implications for development and immunity. *Cell Cycle* **6**, 2138-42 (2007).
21. Tanaka, T., Shibazaki, A., Ono, R. & Kaisho, T. HSP70 mediates degradation of the p65 subunit of nuclear factor kappaB to inhibit inflammatory signaling. *Sci Signal* **7**, ra119 (2014).
22. Subramanian, A. et al. Gene set enrichment analysis: a knowledge-based approach for interpreting genome-wide expression profiles. *Proc Natl Acad Sci U S A* **102**, 15545-50 (2005).

23. Goldberg, A.L. Functions of the proteasome: from protein degradation and immune surveillance to cancer therapy. *Biochem Soc Trans* **35**, 12-7 (2007).
24. Chondrogianni, N. et al. Proteasome activation: An innovative promising approach for delaying aging and retarding age-related diseases. *Ageing Res Rev* **23**, 37-55 (2015).
25. Pandita, T.K. ATM function and telomere stability. *Oncogene* **21**, 611-8 (2002).
26. Sperka, T., Wang, J. & Rudolph, K.L. DNA damage checkpoints in stem cells, ageing and cancer. *Nat Rev Mol Cell Biol* **13**, 579-90 (2012).
27. Sena, L.A., et al. Mitochondria are required for antigen-specific T cell activation through reactive oxygen species signaling. *Immunity* **38**, 225-236 (2013).
28. Buck, M.D., O'Sullivan, D. & Pearce, E.L. T cell metabolism drives immunity. *J Exp Med* **212**, 1345-60 (2015).
29. Groettrup, M., Kirk, C.J. & Basler, M. Proteasomes in immune cells: more than peptide producers. *Nat Rev Immunol* **10**, 73-78 (2010).
30. Kelso, G.F. et al. Selective targeting of a redox-active ubiquinone to mitochondria within cells: antioxidant and antiapoptotic properties. *J Biol Chem* **276**, 4588-96 (2001).
31. Dessolin, J. et al. Selective targeting of synthetic antioxidants to mitochondria: towards a mitochondrial medicine for neurodegenerative diseases? *Eur J Pharmacol* **447**, 155-61 (2002).
32. Devadas, S., Zaritskaya, L., Rhee S.G., Oberley, L., Williams, M.S. Discrete generation of superoxide and hydrogen peroxide by T Cell Receptor stimulation: selective regulation of mitogen-activated protein kinase activation and Fas Ligand expression. *J Exp Med* **195**, 59-70 (2002).
33. Harari, A. et al. Functional signatures of protective antiviral T-cell immunity in human virus infections. *Immunol Rev* **211**, 236-54 (2006).
34. McBride, H.M., Neuspiel, M. & Wasiak, S. Mitochondria: more than just a powerhouse. *Curr Biol* **16**, R551-R560 (2006).
35. Smith-Garvin, J.E., Koretzky, G.A. & Jordan, M.S. T cell activation. *Annu Rev Immunol* **27**, 591-619 (2009).
36. Kumari, S., Curado, S., Mayya, V. & Dustin, M.L. T cell antigen receptor activation and actin cytoskeleton remodeling. *Biochim Biophys Acta* **1838**, 546-56 (2014).
37. Wherry, E.J. et al. Molecular signature of CD8+ T cell exhaustion during chronic viral infection. *Immunity* **27**, 670-84 (2007).
38. Doering, T.A. et al. Network analysis reveals centrally connected genes and pathways involved in CD8+ T cell exhaustion versus memory. *Immunity* **37**, 1130-44 (2012).
39. Kaech, S.M., Hemby, S., Kersh, E. & Ahmed, R. Molecular and functional profiling of memory CD8 T cell differentiation. *Cell* **111**, 837-51 (2002).
40. Bengsch, B. et al. Bioenergetics insufficiencies due to metabolic alterations regulated by the inhibitory receptor PD-1 are an early driver of CD8+ T cell exhaustion. *Immunity* **45**, 358-373 (2016).
41. Petrovas, C. et al. Increased mitochondrial mass characterized the survival defect of HIV-specific CD8+ T cells. *Blood* **109**, 2505-13 (2007).
42. Lopez-Otin, C., Blasco, M.A., Partridge, L., Serrano, M., & Kroemer, G. The hallmarks of aging. *Cell* **153**, 1194-1217 (2013).
43. Ponnappan, S. & Ponnappan, U. Aging and immune function: molecular mechanisms to interventions. *Antioxid Redox Signal* **14**, 1551-85 (2011).
44. Ron-Harel, N., Sharpe, A.H. & Haigis M.C. Mitochondrial metabolism in T cell activation and senescence: a mini-review. *Gerontology* **61**, 131-8 (2015).
45. Sansoni, P. et al. The immune system in extreme longevity. *Exp Gerontol* **43**, 61-5 (2008).
46. O'Sullivan, R.J., Kubicek, S., Schreiber, S.L. & Karlseder, J. Reduced histone biosynthesis and chromatin changes arising from a damage signal at telomeres. *Nat Struct Mol Biol* **17**, 1218-25 (2010).

47. Su, C. et al. DNA damage induces downregulation of histone gene expression through the G1 checkpoint pathway. *EMBO J* **23**, 1133-43 (2004).
48. Cuervo, A.M. & Macian, F. Autophagy and the immune function in aging. *Curr Opin Immunol* **29**, 97-104 (2014).
49. Szklarczyk, R., Nooteboom, M. & Osiewacz, H.D. Control of mitochondrial integrity in ageing and disease. *Philos Trans R Soc Lond B Biol Sci* **369**, 20130439 (2014).
50. Weber, T.A. & Reichert, A.S. Impaired quality control of mitochondria: aging from a new perspective. *Exp Gerontol* **45**, 503-11 (2010).
51. Carreau, A., El Hafny-Rahbi, B., Matejuk, A., Grillon, C. & Kieda, C. Why is the partial oxygen pressure of human tissues a crucial parameter? Small molecules and hypoxia. *J Cell Mol Med* **15**, 1239-1253 (2011).
52. Schurich, A. et al. Distinct metabolic requirements of exhausted and functional virus-specific CD8 T cells in the same host. *Cell Reports* **16**, 1-10 (2016).
53. Dimeloe, S. et al. The immune-metabolic basis of effector memory CD4+ T cell function under hypoxic conditions. *J Immunol* **196**, 106-14 (2016).
54. D'Souza, A.D., Parikh, N., Kaech, S., Shadel, G.S. Convergence of multiple signaling pathways is required to coordinately up-regulate mtDNA and mitochondrial biogenesis during T cell activation. *Mitochondrion* **7**, 374-85 (2007).
55. van der Windt, G.J.W., et al. Mitochondrial respiratory capacity is a critical regulator of CD8+ T cell memory development. *Immunity* **36**, 68-78 (2012).
56. Yi, J.S., Holbrook, B.C., Michalek, R.D., Laniewski, N.G. & Grayson, J.M. Electron transport complex I is required for CD8+ T cell function. *J Immunol* **177**, 852-62 (2006).
57. Buck, M.D., et al. Mitochondrial dynamics controls T cell fate through metabolic programming. *Cell* **166**, 63-76 (2016).
58. Gane, EJ. et al. The mitochondria-targeted anti-oxidant mitoquinone decreases liver damage in a phase II study of hepatitis C patients. *Liver Int* **30**, 1019-1026 (2010).

FIGURE LEGENDS

Figure 1. Gene expression profiling of HBV-specific CD8 T cells from the acute, chronic and resolution phases of hepatitis B infection. (**a**) Representative flow-cytometric analysis profiles of HBV-specific CD8 cells from the indicated patient groups. Left graphs (*pre-sorting*) illustrate the frequency of HBV dextramer-positive cells within the overall CD8 cell population after CD8 cell enrichment with magnetic beads; right graphs (*post-sorting*) document the level of purity of sorted dextramer-positive CD8 cells. (**b**) Hierarchical clustering representation of the 504 genes identified as differentially expressed in HBV-specific CD8 cells from acute (n=5 biological replicates), chronic (n=4) and resolved (n=4) hepatitis B patients by ANOVA and Benjamini-Hochberg correction for multiple testing ($p \leq 0.05$). Data were median-normalized before clustering; up-regulated and down-regulated genes are shown in red and green, respectively. (**c)** Patient group correlation analyzed by Principal Component Analysis (PCA) of ANOVA-filtered data. (**d**) Venn diagram distribution of differentially expressed genes among the three ANOVA patient sub-lists (chronic *vs* resolved, acute *vs* resolved and acute *vs* chronic) determined by post-hoc SNK analysis.

Figure 2. Comparison of chronic and resolved patients by Gene-Set Enrichment Analysis (GSEA). (**a**) List of enriched gene-sets in HBV-specific CD8 cells from chronic and resolved patients identified by GSEA (MSigDB, C2 canonical pathways set). Individual frames identify four distinct functional groups; a representative enrichment plot for each is shown on the right. (**b**) Heat-map representation of differentially expressed genes related to mitochondrion, proteasome, and DNA damage response, which are down-regulated in chronic compared to resolved patients (top three heat-maps); heat-maps of RNA transcription-related genes, down-regulated (*left*) and up-regulated (*right*) in chronic patients are illustrated in the bottom. Most of the up-regulated genes code for negative regulators, including multiple C2H2 zinc finger and KRAB domain-containing proteins and the histone deacetylase HDAC1. Down-regulated genes include various RNA polymerase (I, II and III) subunits, associated general transcription factors (UBTF, TBP, ELOB, ELOA, GTF3C4) and chromatin-related proteins (histones, the NuA4 HAT subunit RUVBL1, SMARCA and the telomere repeat binding factor TERF2IP). Up-

regulated and down-regulated genes are shown in red and green, respectively. Genes were identified by leading edge analyses (a GSEA tool) conducted on each gene-set and were subsequently associated to the functional groups described in (**a**); detailed gene descriptions are available in **Supplementary Table 3**. (**c**) Interaction network (generated by GeneMANIA) of the mitochondrial proteins encoded by genes down-regulated in exhausted CD8 cells from chronic patients. Lines and nodes colors refer to different types of interaction and to the different mitochondrion-related functions of the proteins represented in the network, as indicated.

Figure 3. Mitochondrial dysfunction in chronic HBV patients. (a) Schematics of the mitochondrial components encoded by genes down-regulated in exhausted CD8 cells. (**b)** Bar-plot of the most significantly dysregulated genes related to mitochondria (n=23) and proteasome (n=4; *gray frame*) represented as the ratio between the mean expression values in chronic and resolved patients by microarray (*blue*, HBV-specific CD8 cells) and Nanostring (*red*, HBV-specific CD8 cells; *green*, PD1+ HBV-specific CD8 cells; *black*, PD1+ total CD8 cells). Four chronic and four resolved patients were analyzed by microarrays; three different chronic and three different resolved patients by Nanostring. **(c)** Percent of MMP depolarized virus-specific CD8 cells measured by JC1- and DiOC6 staining after overnight anti-CD3 stimulation. **(d)** Mitochondrial mass variation of virus-specific CD8 cells is expressed as the ratio of MitoTracker Green MFI in anti-CD3 stimulated *versus* non-stimulated cells. **(e)** Mitochondrial superoxide levels are presented as MitoSOX Red MFI in unstimulated dextramer+ cells (Mann-Whitney-U test) and as MFI variations in anti-CD3 stimulated and unstimulated cells from healthy controls (*left*), resolved (*middle*) and chronic (*right*) patients, respectively (Wilcoxon-matched-paired test).

Figure 4. Correction of mitochondrial dysfunction by MT-antioxidants (a) Percent of depolarized CD8 cells from chronic patients measured by JC-1 staining, after overnight HBV-core peptide stimulation in the presence or absence of MitoQ (Wilcoxon-matched-paired test). **(b)** Superoxide levels in unstimulated and HBV-core peptide stimulated cells cultured in the presence or absence of MT-antioxidants. Results from 6 chronic patients are illustrated. (**c**) Cumulative ETC protein levels in untreated and MitoQ-treated *(*MTQ*, left)* or MitoTempo-

treated *(*MTT, *right)* HBV-specific CD8 cells derived from cultures stimulated for 10 days with the core peptide.

Figure 5. Functional restoration of exhausted HBV-specific T cells by MT- antioxidants. (**a**) Percentage of IFNγ-positive, TNFα-positive and double-positive IFNγ+TNFα+ CD8 cells in short-term T-cell lines (n=27) generated by HBV-core peptide stimulation in the presence or absence of MitoQ (MTQ, *top*) or MitoTempo (MTT, *bottom*). Median, 25^{th} and 75^{th} percentiles, minimum and maximum values of responses to MT-antioxidant treatment are shown in the box-and-whisker plots on the *left* (statistics by the Wilcoxon-matched-paired test)*;* grey boxes represent IFNγ levels of reference CD8 cells from resolved patients (n=8). MT antioxidant-induced variations (*fold-increase*) of cytokine levels in CD8 cells from individual chronic patients are shown in the *middle* graphs; median fold-increase values are reported (statistics by the Wilcoxon-signed-rank test). Representative dot-plots illustrating IFNγ- and TNFα-positive cells in the presence or absence of MT-antioxidants are shown on the *right*. (**b**) Fold-increase in cytokine levels upon MT-antioxidant treatment (MTQ and MTT in the *top* and *bottom* panels, respectively) analyzed in the global CD3+ T cell population following HBV-core peptide stimulation **(c)** MitoQ-induced fold-increase of cytokine levels in CD8 and CD4 T cells isolated from the liver of 6 chronic patients (*left*). Note that at least a single T-cell subset (either CD8 or CD4) was responsive to MitoQ in each patient. Representative dot-plots illustrating cytokine production in untreated and MitoQ-treated paired peripheral and intrahepatic T cell samples from two chronic patients are shown on the right. *Top*: cytokine production by peptide-stimulated dextramer+ CD8 cells; *bottom*: cytokine production by HBV peptide-stimulated CD4 cells; gating strategies are also illustrated.

Figure 6. Specificity of the MT-antioxidant effect on cytokine production. (a) Fold increases in cytokine production in paired samples of MT-antioxidant treated HBV-specific and FLU-specific CD8 T cells from the same HLA-A2+ chronic patients (n=9). Representative ICS experiments showing the effect of both MT-antioxidants on HBV- and FLU-specific CD8 cells from the same chronic hepatitis B patient are illustrated. For each of the three experimental conditions (*no antioxidant*, *MitoQ* and *MitoTempo*), the graphs on the *left* show the frequency of dextramer-positive cells of the indicated specificity, while those on the *right* show the

frequency of IFNγ producing, dextramer-positive CD8 cells after specific peptide stimulation. (**b**) T cell cultures (n=9) were generated by anti-CD3 stimulation in the presence or absence of MT-antioxidants, in order to distinguish between a global and a HBV-specific effect of MitoQ (*top*) and MitoTempo (*bottom*). Results are expressed as box-and-whisker plots reporting median, 25^{th} and 75^{th} percentiles, minimum and maximum values of cytokine-producing CD8 or CD3 cells following anti-CD3 stimulation in the presence or absence of MT-antioxidants. (**c**) MT-antioxidants-induced fold changes in IFNγ and TNFα production in 27 chronic HBV patients and in 12 patients with resolved infection.

ONLINE METHODS

Study subjects. The following groups of patients were enrolled into the study at the Unit of Infectious Diseases and Hepatology of the Azienda Ospedaliero-Universitaria of Parma, Italy, and at the Unit of Infectious Diseases, Arcispedale SMN of Reggio Emilia, Italy.

- 42 treatment-naïve patients with HBeAg-negative, chronic active hepatitis B; diagnosis was based on ALT elevation lasting for more than 6 months, plus HBsAg, anti-HBc, anti-HBe and HBV-DNA positivity (**Supplementary Table 4**). 27 patients were HLA-A2-positive (+); screening for HLA-A2 was performed by Peripheral Blood Mononuclear Cell (PBMC) staining with a fluorescent anti-HLA-A2.01 antibody (BD Biosciences, San Jose, CA).
- 8 HLA-A2+ patients (aged 24 to 44 years, median 37) with clinical, biochemical, and virological evidence of acute HBV infection (ALT range: 201-1785 U/L), including transaminase levels at least 10 times higher than the normal upper limit and serum detection of HBsAg and anti-HBc IgM antibodies.
- 24 (12 HLA-A2+) subjects who spontaneously recovered from acute HBV infection (HBsAg-negative, anti-HBs+, aged 24-68, median 37.5), 6-10 months after the peak of ALT elevation.
- 16 HLA-A2+ healthy subjects (aged 25-51, median 34), as controls.

All patients were negative for anti-hepatitis C virus, delta virus, human immunodeficiency virus type 1 (HIV-1) and type 2 (HIV-2) antibodies and for other markers of viral or autoimmune hepatitis. No randomization was used to determine patient groups and during all experiments investigators were not blinded to the group allocation. The study was approved by the Ethical Committee of the Azienda Ospedaliero-Universitaria of Parma, Italy, and all subjects provided written, informed consent.

Synthetic peptides, peptide-HLA class I dextramers, and antibodies. 42 15-mer synthetic peptides overlapping by 10 amino acid (aa.) residues and covering the entire sequence of the core protein of genotype D HBV (Chiron Mimotopes, Victoria, Australia) were pooled into a single mixture and used in functional validation experiments performed in HLA-A2 negative patients. Peptides covering the HLA-A2-restricted epitopes of the HBV core (aa. 18-27: FLPSDFFPSV) and envelope (aa. 183-191: FLLTRILTI; 335-343. WLSLLVPFV; and 348-357: GLSPTVWLSV) proteins of HBV genotype D, cytomegalovirus (CMV) pp65

(NLVPMVATV) and influenza virus (FLU) matrix (GILGFVFTL) were purchased from Proimmune (Oxford, UK), and the corresponding PE- or APC-labeled dextramer peptide-HLA class I complexes from Immudex (Copenhagen, Denmark). The entire set of HBV peptides and dextramers was used to detect virus-specific CD8 cells in PBMC and liver. Since envelope specific CD8 cells were never detected in HLA-A2 positive chronic HBV patients, only the HBV core 18-27 peptide and the corresponding dextramer were used for validation experiments. Anti-CD3-BD Horizon™ PE-CF594 (clone HCHT1), CD8-PE-Cy7 (cat.# 557746), CD4-PE (cat.# 555347), IFNγ-Alexa Fluor®700 (clone B27), CD45-FITC (cat.# 555482), (BD Biosciences-Pharmingen), CD3-APC/Cy7 (clone SK7), CD279 (PD1) PE-Cy7 (clone EH12.2H7), anti-Cytochrome C-Alexa Fluor®647 (clone 6H2.B4) (Biolegend, San Diego, Ca), TNFα-FITC (clone cA2, Miltenyi Biotec, Bergisch Gladbach, Germany), anti-ATP5O-Alexa Fluor®488 (clone 4C11C10D12) (Abcam, Cambridge, UK), Annexin V-APC and the viability probe 7-AAD (BD Biosciences) were used for T cell staining. LEAF purified anti-CD3 (clone HIT3a, Biolegend) was used for T cell stimulation.

Isolation of Peripheral Blood Mononuclear Cells (PBMC) and Liver Infiltrating Lymphocytes (LIL). PBMCs were isolated from fresh heparinized blood by Ficoll-Hypaque density gradient centrifugation and cryopreserved in liquid nitrogen until the day of analysis. LIL were isolated from excess liver tissue not needed for diagnostic purposes. The liver biopsy fragment was extensively washed in RPMI to remove contaminating blood and digested with collagenase (Sigma Chemical Co, St. Louis, MO; 1 μg/mL) and DNAase (Sigma Chemical Co; 25 μg/mL) for 1 hour, at 37°C. The mononuclear cell suspension was then washed and resuspended in complete medium. After isolation, lymphocytes were cultured in a round-bottomed 96-well plate (at least 20,000 LIL/well), in the presence of autologous irradiated (4000 rads) PBMC (1 x 10^5/well) and HBV peptides; after 3 days, activated T cells were expanded by addition of IL-2 (50 U/mL).

Sorting. After thawing of PBMCs, CD8+ T cells were isolated with the CD8+ T Cell Isolation Kit (Miltenyi Biotec) and labeled with 7-AAD, anti-CD45, anti-CD3, anti-CD8, and HLA-Class I dextramers in order to identify antigen-specific T cell sub-populations. CD8+ dextramer+ cells (about 1000 cells/sample) were subsequently sorted with a FACSAria III Cell Sorter (BD Biosciences). For Nanostring experiments, cells were labeled with 7-AAD, anti-

CD3, anti-CD8, anti-CD279 (PD1) antibodies and HLA-Class I dextramers; 10 cells/sample were collected directly in Single Cell Lysis Solution (Life Technologies, Carlsbad, CA).

Microarray data acquisition. RNA was purified from dextramer-sorted human CD8+ T cells with the Nucleospin® RNA XS kit (Macherey Nagel, Duren, Germany) according to the manufacturer's instructions. Total RNA concentration was determined with a Nanodrop spectrophotometer and/or with the Ribogreen RNA quantification kit (Molecular Probes, Life Technologies). RNA integrity was evaluated with a Bioanalyzer 2100 traces system (Agilent Technologies, Santa Clara, CA). Total RNA was amplified with the Transplex Whole Transcriptome Amplification (WTA2) kit (Sigma-Aldrich, St.Louis, Mo) and purified with GenElute™ PCR Clean-Up silica spin-colums (Sigma) as per manufacturer's instructions. cDNA was labeled with the ULS Fluorescent Labeling kit (Agilent Technologies) and hybridized to 60-mer oligonucleotide Whole Human Genome Microarrays (Human GE 4x44K v2, Agilent Technologies), following the manufacturer's protocol. Microarray slides were scanned with an Agilent dual-laser DNA microarray scanner. The Agilent Feature Extraction software with default settings (user manual version 7.5) was used to obtain normalized expression values from the raw scans.

Microarray data analysis. The software package GeneSpring GX v11.5 (Agilent Technologies) was used for quality control checks, data normalization by the quantile method, and initial microarray data analysis. Probes detectable in at least three replicates for each condition were retained for further analysis. ANOVA with the Benjamini-Hochberg correction for multiple testing (FDR $\leq$0.05) was used to track genes differentially expressed between acute, chronic and resolved patients. Genes differentially expressed between the three groups were identified by Student–Newman–Keuls (SNK) post-hoc analysis. Hierarchical clustering and heat map visualization of the data were generated with GeneSpring. A Self Organizing Maps algorithm[16] with a hexagonal grid topology, an analytical tool less error-prone than hierarchical clustering methods[59], was applied to the ANOVA-filtered gene set to obtain an unsupervised visualization of the gene clusters coordinately expressed among the different patients' groups. Enrichment analysis was then performed on each cluster with the use of WebGestalt (WEB-based GEne SeT AnaLysis Toolkit) and DAVID (Database for Annotation, Visualization, and Integrated Discovery)[60,61] in order to pinpoint significantly enriched pathways or gene ontology terms. Parallel identification of pathways significantly enriched in

exhausted HBV-specific CD8 cells compared to control cells was performed by Gene Set Enrichment Analysis (GSEA)[22], as it allows to uncover sets of functionally related genes, rather than individual high-scoring genes above an arbitrarily set cutoff. In addition, by focusing on all detected (above-background) genes, GSEA is less biased and more sensitive, thus allowing to detect even subtle enrichment signals. GSEA was also used to compare our gene expression profiles with those of previously published, related studies. To this end, we used the Molecular Signature Database v 4.0 (CP, canonical pathways; C5, GO gene sets; C7, Immunologic signatures gene sets) with the permutation type set to 'gene set' to calculate statistical significance, as suggested for less than seven replicates; default settings were applied to all the other options. The GeneMANIA prediction server[62] was used for network analysis. The results of GSEA for the chronic *vs.* resolved and chronic *vs.* healthy comparisons were visualized as networks (enrichment maps) using the Cytoscape software[63]. Expression data are available at NCBI GEO: GSE67801.

Quantitative PCR. Expression levels of a subset of modulated genes were independently determined by Taqman gene expression assays (Life Technologies) using the same amplified cDNAs utilized for microarray analysis as starting material. The selected genes included PDCD1 (assay Hs00169472_m1), CD244 (assay Hs00900277_m1), BATF (assay Hs00232390_m1), ATP5D (Hs00961522_g1) HSPA1L (Hs00271466_s1), HSPA1A (Hs04187663_g1), PSMB8 (Hs00544758_m1) and NDUFA6 (Hs00899690_m1); GAPDH (Hs02758991_g1) served as a loading and normalization control. The expression levels of nine additional genes - KLRG1 (assay Hs.PT.56a.2949117), EOMES (Hs.PT.56a.27752441), TBX21 (Hs.PT.56a.20216516), CD28 (Hs.PT.56a.24318159), TIMM23 (Hs.PT.58.50457315), TIMM10 (Hs.PT.58.27750266), PSMD4 (Hs.PT.58.45566355), CTLA4 (5'UTR-EX1 custom: F: 5-TCCTTGATTCTGTGTGGGTTC-3, R: 5-TTTATGGGAGCGGTGTTCAG-3, probe: 5-ACACATTTCAAAGCTTCAGGATCCTGA-3) and SUMO1 (Hs.PT.58.26957310) - were determined by PrimeTime® qPCR 5' Nuclease Assays (IDT, Coralville, IA) using the relative quantification method; also in this case, GAPDH served as a reference housekeeping gene (**Supplementary Fig. 5, 7**).

Staining of mitochondrial Electron Transport Chain (ETC) proteins. After surface staining, cells were fixed with Cytofix/Cytoperm solution (BD Biosciences) and permeabilized with 0.5% Triton X-100 (Sigma-Aldrich, St. Louis, Mo); anti-Cytochrome C and anti-ATP5O

monoclonal antibodies were then added and incubated for 15 min at room temperature in the dark. Results were expressed as median fluorescence intensity (MFI) of dextramer-positive cells.

Mitochondrial membrane potential, mitochondrial mass and mitochondrial superoxide assays. Mitochondrial membrane potential (MMP) was determined on PBMCs incubated overnight in anti-CD3-coated (10 µg/ml anti-CD3 mAb) or uncoated tissue culture plates using the potentiometric probes JC-1 and DiOC6(3) (3,3'-Dihexyloxacarbocyanine Iodide) (Molecular Probes, Life Technologies). After surface staining, cells were incubated with JC-1 (2.5 µg/ml) or DiOC6(3) (20 nM) for 15 min at 37°C, and protected from light before flow-cytometric analysis. Samples were acquired on FACSCANTO II multicolor flow cytometer and were analyzed with the DIVA software (BD Biosciences). The decrease in JC-1 or DiOC6 fluorescence caused by co-treatment (15 min at 37°C) with the protonophores valinomycin or carbonyl cyanide m-chlorophenyl hydrazine (CCCP) (Molecular Probes) served as a positive control for MMP depolarization. Dextramer+ virus-specific depolarized cells were quantified by subtracting the percentage of $FL1^{high}FL2^{low}$ cells (JC-1 stainings) or $FL1^{low}$ cells (DiOC6 stainings) detected in the unstimulated samples from the percentage of the corresponding cell subsets detected in the stimulated samples. For mitochondrial mass measurement, cells were surface- stained, then incubated with MitoTracker Green FM (Molecular Probes) (100 nM) for 15 min at 37°C and finally acquired by flow cytometry.

Mitochondrial mass changes in virus-specific cells were determined after anti-CD3 stimulation and expressed as the ratio between the MitoTracker Green (FL1) median fluorescence intensity (MFI) of overnight anti-CD3 stimulated and unstimulated samples.

Mitochondrial superoxide levels in virus-specific cells were determined, after cell surface staining, by incubation (15 min at 37°C) of overnight anti-CD3 stimulated and unstimulated cells in the presence of MitoSOX Red (5µM; Molecular Probes).

Aggresome detection. For the detection of aggregates, after overnight PBMC stimulation with coated anti-CD3, cells were surface stained and then the ProteoStat® Aggresome Detection Kit (Enzo Life Sciences, New York, NY) was used according to the manufacturer's protocol, before flow cytometry acquisition. Cells treated with 5 µM of proteasome inhibitor (MG-132) served as

positive controls. Aggresome activity factor values are expressed as the ratio of ProteoStat median fluorescence intensity (MFI) between stimulated and unstimulated samples.

Nanostring analysis. Single Cell Lysis Solution (Life Technologies) was used to extract RNA from 10 sorted cells. Converted cDNA (SuperScript® VILO MasterMix, Life Technologies) was used for each NanoString assay, which was performed according to the manufacturer's protocols ("nCounter XT Gene Expression assay for single cells"). The gene probe set was selected from the custom probe set used, and housekeeping genes (EEF1G, GAPDH, POLR2A, PPIA, RPL19) were added for data normalization. The list of genes represented in our custom code set is provided as follows: ASAH2 (**Accession #** NM_019893.2), ATP5D (NM_001687.4), ATP5J (NM_001003703.1), ATP5J2 (NM_004889.2), ATP6V0C (NM_001198569.1), COX5B (NM_001862.2), COX6A1 (NM_004373.2), CPT1A (NM_001876.3), CYCS (NM_018947.4), FIS1 (NM_016068.2), LRPPRC (NM_133259.3), MRPS11 (NM_176805.2), NDUFA4 (NM_002489.2), NDUFA5 (NM_005000.2), NDUFA6 (NM_002490.3), PHB2 (NM_007273.3), PSEN1 (NM_000021.2), SLC25A1 (NM_005984.2), SLC25A5 (NM_001152.3), TCIRG1 (NM_006053.2), TFAM (NM_003201.1), TIMM23 (NM_006327.2), UQCRC1 (NM_003365.2), PSMC4 (NM_006503.2), PSMD3 (NM_002809.2), PSME1 (NM_006263.2), SEC61A1 (NM_013336.3).

T-cell expansion, MT-antioxidant treatment and cytokine production assays. Short-term T-cell lines were generated by 10 days stimulation of PBMCs with HBV-core peptides or HLA-A2-restricted peptides (each at a final 1 μM concentration) in the presence or absence of MitoQ (0.1 μM; kindly provided by Dr. Michael P. Murphy, MRC Mitochondrial Biology Unit, Cambridge, UK) or MitoTempo (10 μM; Sigma). For total CD3+ lymphocyte stimulation experiments, PBMCs were added to anti-CD3 pre-coated wells in the presence or absence of MT antioxidants. At the end of the culture period, cytokine determinations (IFNγ and TNFα) were performed by intracellular cytokine staining (ICS) as described previously[11].

Statistical analysis. The GraphPad Prism software was used for statistical analysis. Correlations between microarray and qPCR data were evaluated by the Spearman's rank correlation test. After checking that variance between groups was not significantly different (F

test), Mann-Whitney U test was applied to compare percentages of depolarized virus-specific CD8 upon anti-CD3 stimulation. Cytokine production levels in the different experimental conditions were compared by the Wilcoxon matched paired test. Before every comparison normality distribution of data was tested by the Kolmogorov–Smirnov test, and non-parametric statistic was applied. Fold changes (FC) in cytokine production upon mt-antioxidant treatments (FC ≠ 1) were evaluated by the Wilcoxon signed rank tests. All tests were two-tailed.

METHODS REFERENCES

59. Zhang, J.& Hai Fang in *Applications of Self-Organizing Maps* (ed. Johnsson, M.), 181–204 (In Tech, Rijeka, Croatia, 2012).
60. Huang da, W., Sherman, B.T. & Lempicki, R.A. Bioinformatics enrichment tools: paths toward the comprehensive functional analysis of large gene lists. *Nucleic Acids Res* **37**, 1-13 (2009).
61. Wang, J., Duncan, D., Shi, Z. & Zhang, B. WEB-based GEne SeT AnaLysis Toolkit (WebGestalt): update 2013. *Nucleic Acids Res* **41**, W77-83 (2013).
62. Warde-Farley, D. et al. The GeneMANIA prediction server: biological network integration for gene prioritization and predicting gene function. *Nucleic Acids Res* **38**, W214-20 (2010).
63. Saito, R. et al. A travel guide to Cytoscape plugins. *Nat Methods* **9**, 1069-76 (2012).

a

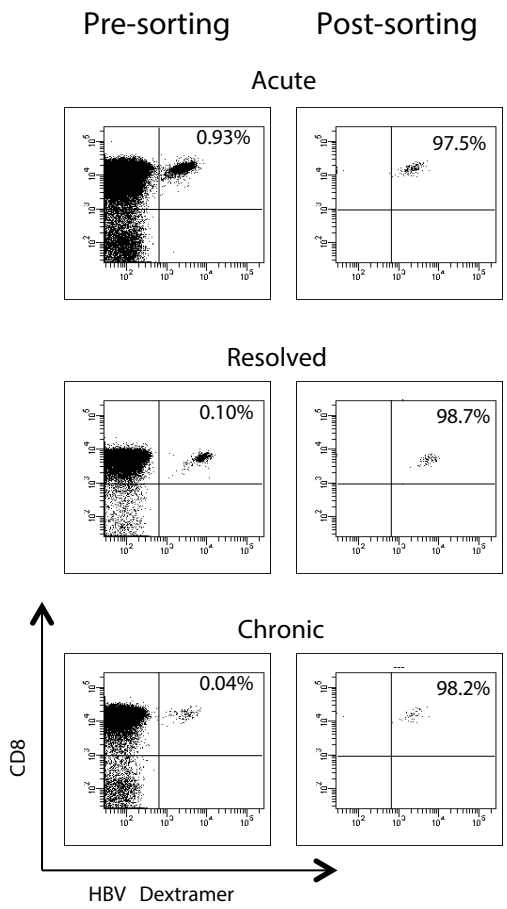
Pre-sorting
Post-sorting
Acute
0.93%
97.5%
Resolved
0.10%
98.7%
Chronic
0.04%
98.2%
CD8
HBV Dextramer

b

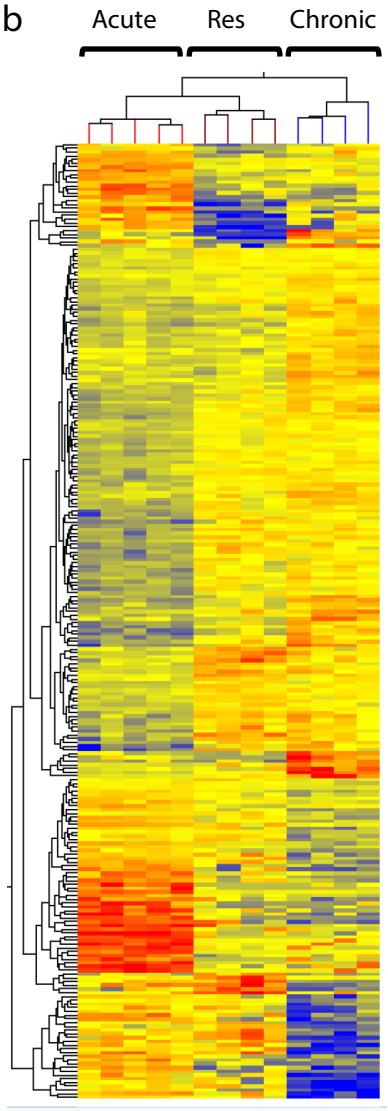
Acute
Res
Chronic

c

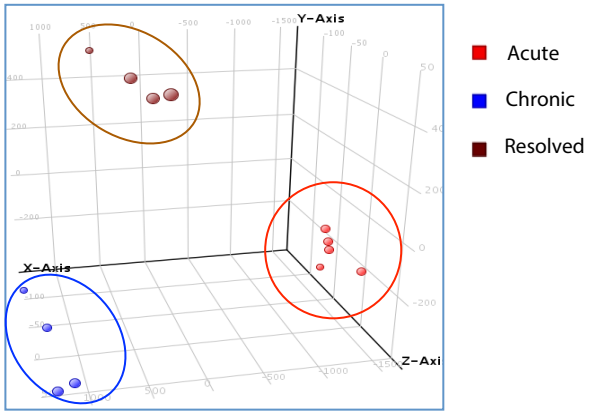
Y-Axis
X-Axis
Z-Axi
Acute
Chronic
Resolved

d

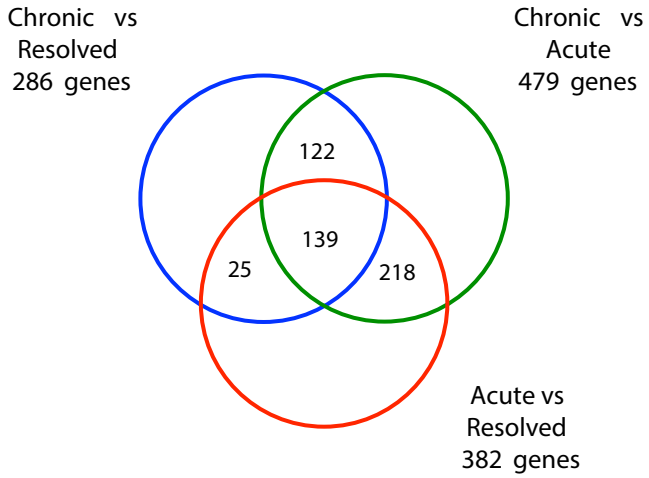
Chronic vs Resolved 286 genes
Chronic vs Acute 479 genes
Acute vs Resolved 382 genes
122
139
25
218

NAME	NES	NOM p-val	FDR q-val
REACTOME_RESPIRATORY ELECTRON TRANSPORT ATP SYNTHESIS BY CHEMIOSMOTIC COUPLING AND HEAT PRODUCTION BY UNCOUPLING PROTEINS	-2.006	$< 10^{-4}$	0.0094
REACTOME_RESPIRATORY ELECTRON TRANSPORT	-1.855	$< 10^{-4}$	0.0343
KEGG_OXIDATIVE PHOSPHORYLATION	-1.693	0.0022	0.0958
KEGG_PROTEASOME	-2.059	$< 10^{-4}$	0.0061
REACTOME_P53 DEPENDENT G1 DNA DAMAGE RESPONSE	-1.988	$< 10^{-4}$	0.0096
REACTOME_P53 INDEPENDENT G1 S DNA DAMAGE CHECKPOINT	-1.922	$< 10^{-4}$	0.022
REACTOME_RNA POL I PROMOTER OPENING	-2.414	$< 10^{-4}$	$< 10^{-4}$
REACTOME_RNA POL I RNA POL III AND MITOCHONDRIAL TRANSCRIPTION	-2.153	$< 10^{-4}$	0.0025
REACTOME_RNA POL I TRANSCRIPTION	-2.074	$< 10^{-4}$	0.0048
REACTOME_TRANSCRIPTION	-1.966	$< 10^{-4}$	0.0123
REACTOME_DEPOSITION OF NEW CENPA CONTAINING NUCLEOSOMES AT THE CENTROMERE	-1.922	$< 10^{-4}$	0.0099
REACTOME_PACKAGING OF TELOMERE ENDS	-1.996	$< 10^{-4}$	0.0104
REACTOME_ER PHAGOSOME PATHWAY	-2.036	$< 10^{-4}$	0.007
REACTOME_REGULATION OF ORNITHINE DECARBOXYLASE	-1.777	$< 10^{-4}$	0.058
KEGG_SYSTEMIC LUPUS ERYTHEMATOSUS	-1.78	$< 10^{-4}$	0.058
REACTOME_SIGNALING BY THE B CELL RECEPTOR BCR	-1.73	0.0022	0.082
REACTOME_ENOS ACTIVATION AND REGULATION	-1.708	0.0195	0.0864

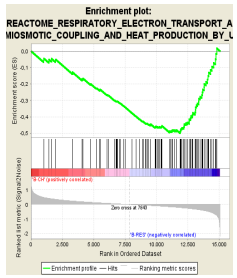

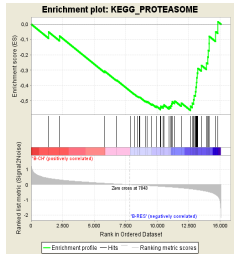

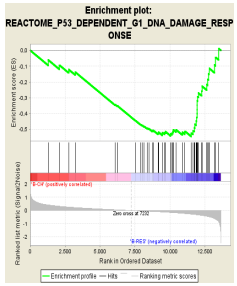

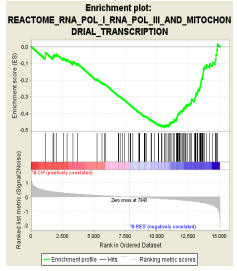

b

MITOCHONDRION

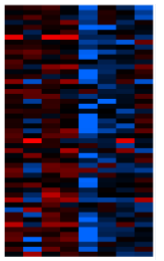

PROTEASOME

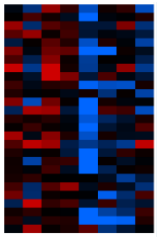

DNA DAMAGE RESPONSE

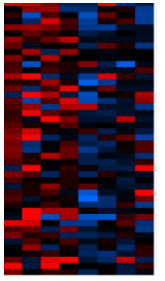

Res Chr

TRANSCRIPTION

down up

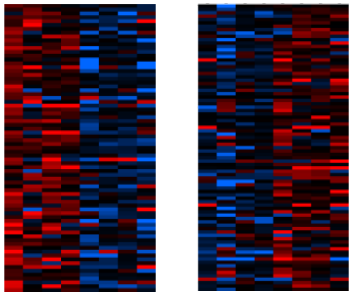

Res Chr Res Chr

-5 0 5

c

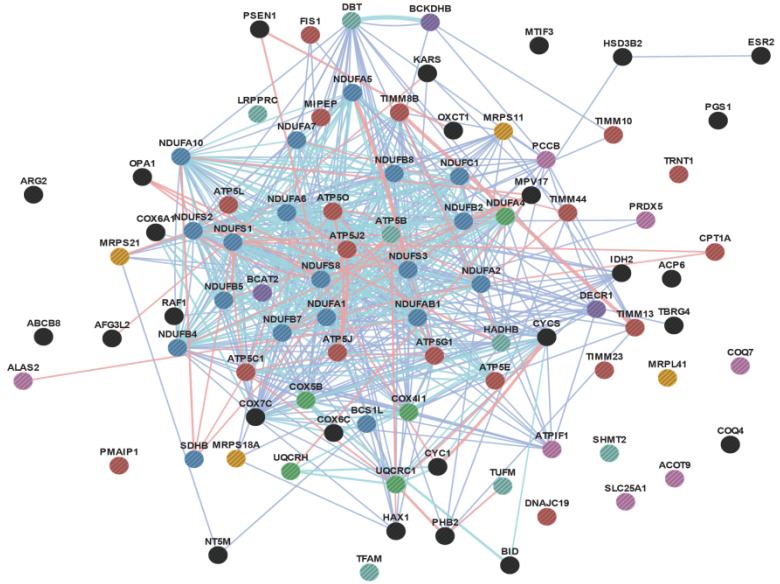

Networks legend

- Co-localization
- Pathway
- Physical interactions

Functions legend

- mitochondrial nucleoid
- cofactor metabolic process
- mitochondrial transport
- proton transport
- organic acid catabolic process
- mitochondrial ribosome
- mitochondrial respiratory chain
- query genes

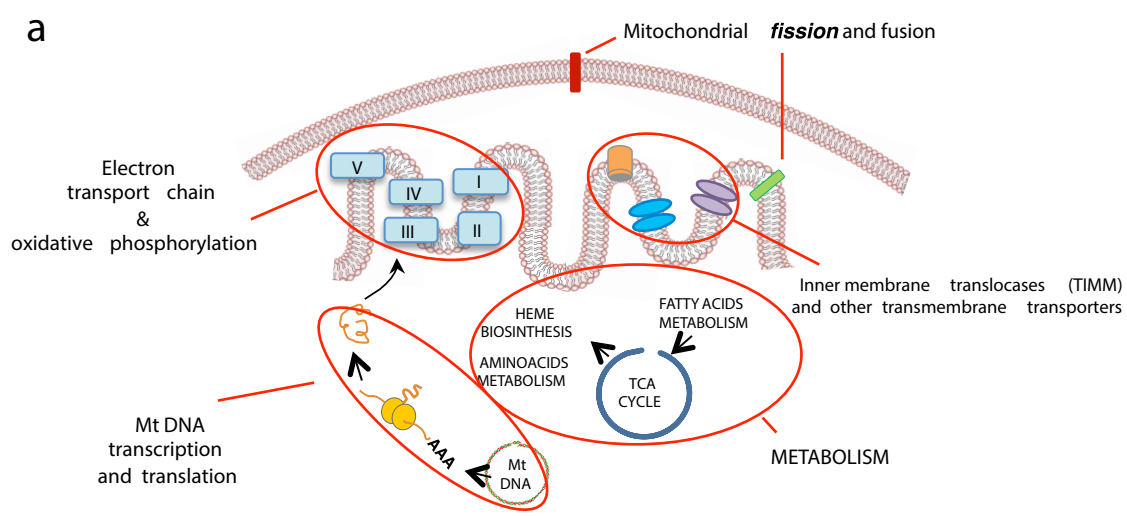
a
Mitochondrial fission and fusion
Electron transport chain & oxidative phosphorylation
V
IV
III
I
II
Inner membrane translocases (TIMM) and other transmembrane transporters
HEME BIOSINTHESIS
FATTY ACIDS METABOLISM
AMINOACIDS METABOLISM
TCA CYCLE
Mt DNA transcription and translation
AAA
Mt DNA
METABOLISM

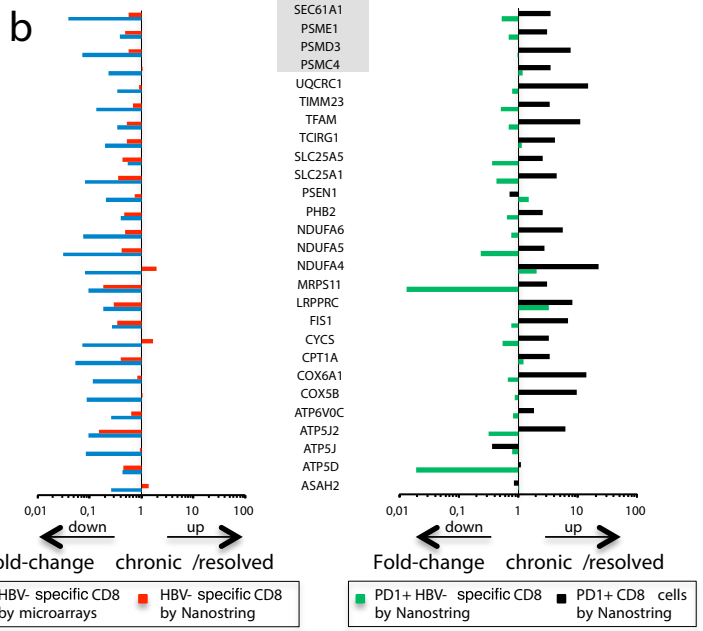
b
SEC61A1
PSME1
PSMD3
PSMC4
UQCRC1
TIMM23
TFAM
TCIRG1
SLC25A5
SLC25A1
PSEN1
PHB2
NDUFA6
NDUFA5
NDUFA4
MRPS11
LRPPRC
FIS1
CYCS
CPT1A
COX6A1
COX5B
ATP6V0C
ATP5J2
ATP5J
ATP5D
ASAH2
0,01 0,1 1 10 100
down up
Fold-change chronic /resolved
HBV- specific CD8 by microarrays
HBV- specific CD8 by Nanostring
PD1+ HBV- specific CD8 by Nanostring
PD1+ CD8 cells by Nanostring

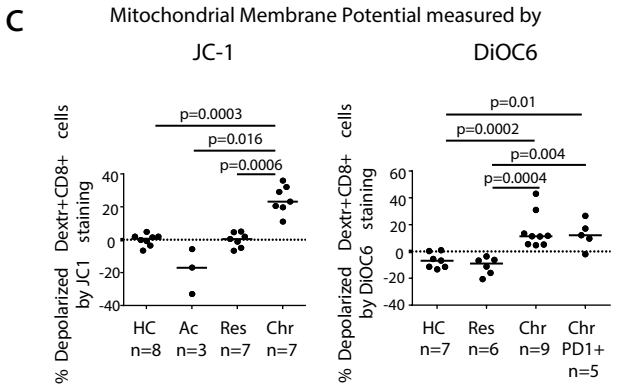
c
Mitochondrial Membrane Potential measured by
JC-1
DiOC6
% Depolarized Dextr+CD8+ cells by JC1 staining
p=0.0003
p=0.016
p=0.0006
HC n=8
Ac n=3
Res n=7
Chr n=7
% Depolarized Dextr+CD8+ cells by DiOC6 staining
p=0.01
p=0.0002
p=0.004
p=0.0004
HC n=7
Res n=6
Chr n=9
Chr PD1+ n=5

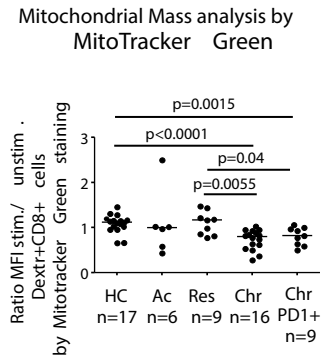
d
Mitochondrial Mass analysis by
MitoTracker Green
Ratio MFI stim./ unstim . Dextr+CD8+ cells by Mitotracker Green staining
p=0.0015
p<0.0001
p=0.04
p=0.0055
HC n=17
Ac n=6
Res n=9
Chr n=16
Chr PD1+ n=9

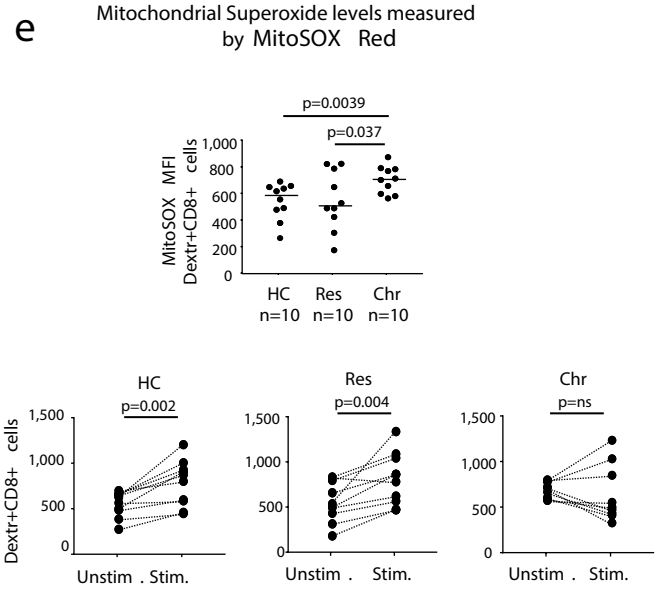
e
Mitochondrial Superoxide levels measured by MitoSOX Red
MitoSOX MFI Dextr+CD8+ cells
p=0.0039
p=0.037
HC n=10
Res n=10
Chr n=10
HC
p=0.002
Res
p=0.004
Chr
p=ns
Unstim . Stim.

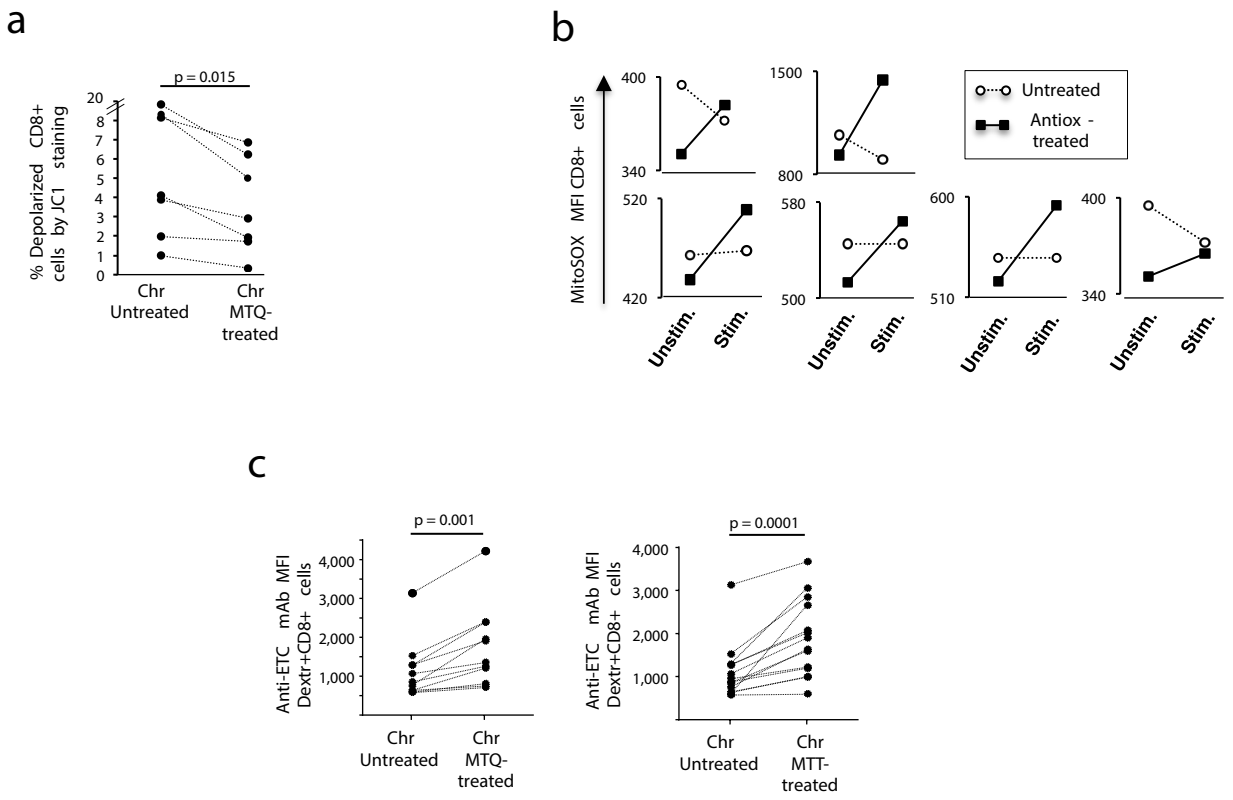
a
p = 0.015
% Depolarized CD8+ cells by JC1 staining
20
8
7
6
5
4
3
2
1
0
Chr Untreated
Chr MTQ-treated
b
MitoSOX MFI CD8+ cells
400
340
1500
800
520
420
580
500
600
510
400
340
Unstim.
Stim.
Untreated
Antiox - treated
c
p = 0.001
Anti-ETC mAb MFI Dextr+CD8+ cells
4,000
3,000
2,000
1,000
Chr Untreated
Chr MTQ-treated
p = 0.0001
Anti-ETC mAb MFI Dextr+CD8+ cells
4,000
3,000
2,000
1,000
Chr Untreated
Chr MTT-treated

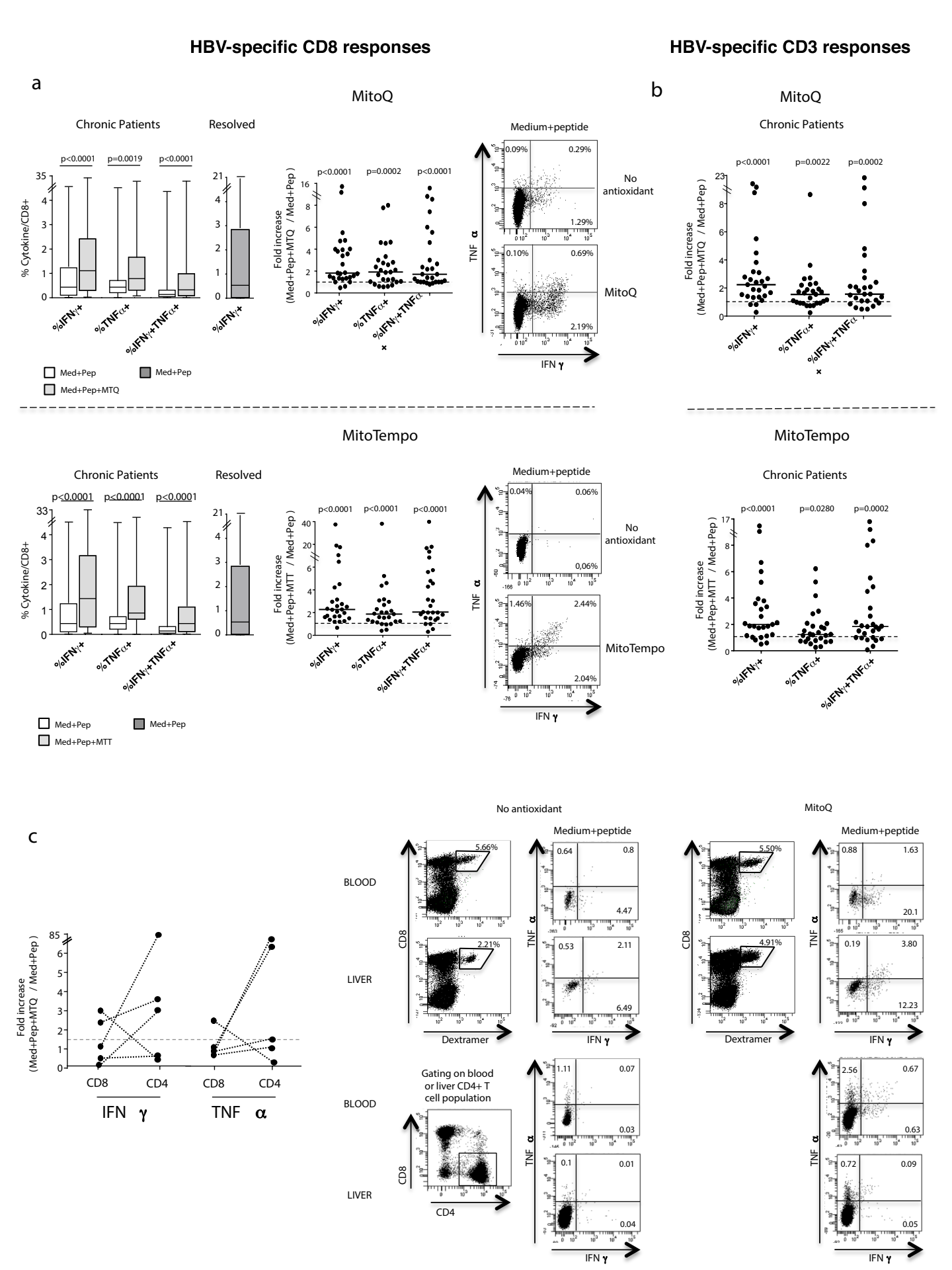
HBV-specific CD8 responses
HBV-specific CD3 responses
a
b
c
MitoQ
MitoTempo
Chronic Patients
Resolved
% Cytokine/CD8+
Fold increase (Med+Pep+MTQ / Med+Pep)
Fold increase (Med+Pep+MTT / Med+Pep)
p<0.0001
p=0.0019
p<0.0001
p<0.0001
p=0.0002
p<0.0001
p=0.0022
p=0.0002
p<0.0001
p=0.0280
p=0.0002
%IFNγ+
%TNFα+
%IFNγ+TNFα+
Med+Pep
Med+Pep+MTQ
Med+Pep+MTT
Medium+peptide
No antioxidant
MitoQ
MitoTempo
TNF α
IFN γ
0.09%
0.29%
1.29%
0.10%
0.69%
2.19%
0.04%
0.06%
0,06%
1.46%
2.44%
2.04%
Fold increase (Med+Pep+MTQ / Med+Pep)
CD8
CD4
IFN γ
TNF α
BLOOD
LIVER
Dextramer
Gating on blood or liver CD4+ T cell population
5.66%
2.21%
5.50%
4.91%
0.64
0.8
4.47
0.53
2.11
6.49
0.88
1.63
20.1
0.19
3.80
12.23
1.11
0.07
0.03
0.1
0.01
0.04
2.56
0.67
0.63
0.72
0.09
0.05

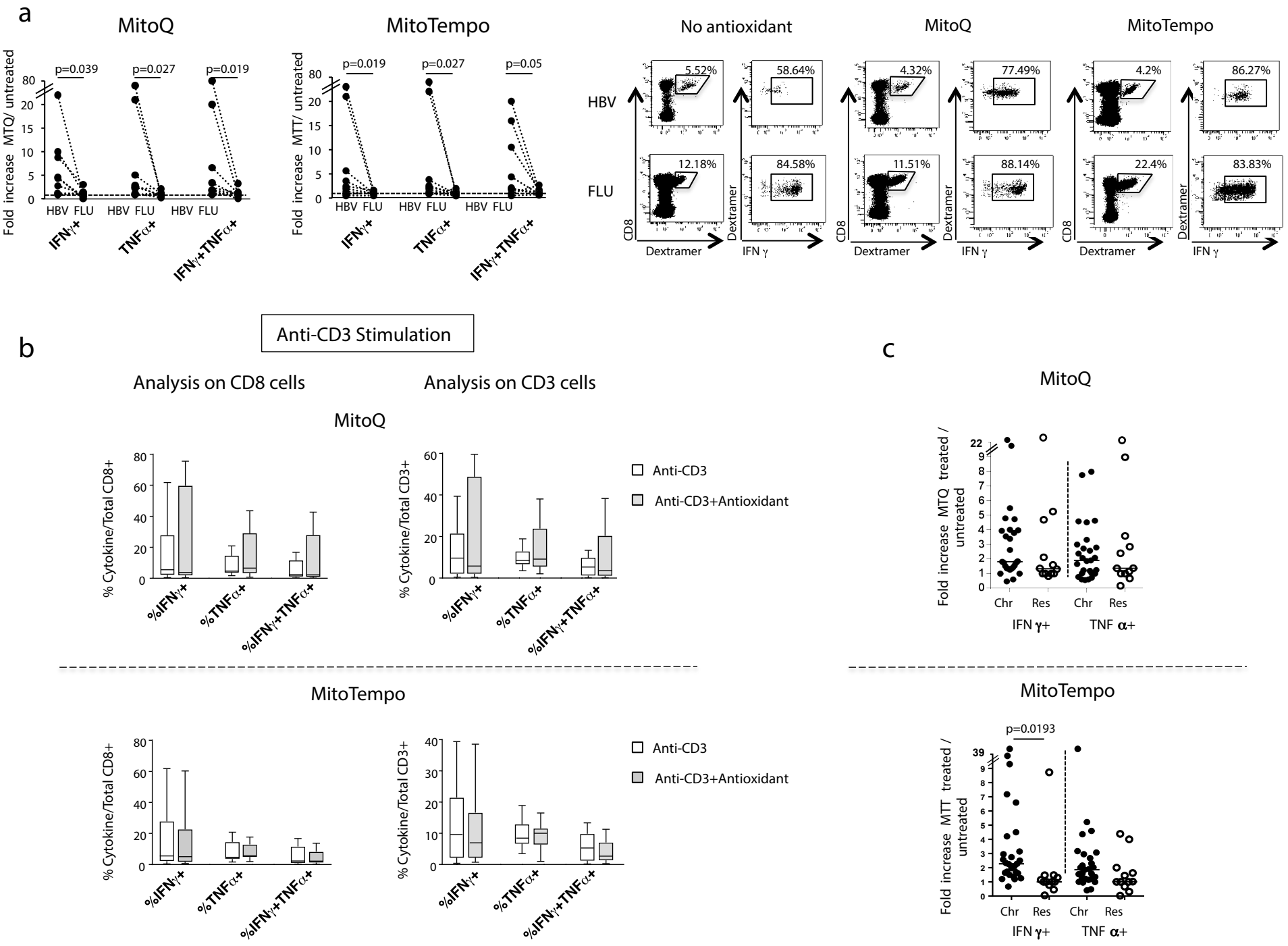
a
MitoQ
MitoTempo
No antioxidant
MitoQ
MitoTempo
Fold increase MTQ/ untreated
Fold increase MTT/ untreated
p=0.039
p=0.027
p=0.019
p=0.019
p=0.027
p=0.05
HBV FLU
IFNγ+
TNFα+
IFNγ+TNFα+
HBV
FLU
5.52%
58.64%
4.32%
77.49%
4.2%
86.27%
12.18%
84.58%
11.51%
88.14%
22.4%
83.83%
CD8
Dextramer
IFN γ
b
Anti-CD3 Stimulation
Analysis on CD8 cells
Analysis on CD3 cells
MitoQ
MitoTempo
% Cytokine/Total CD8+
% Cytokine/Total CD3+
%IFNγ+
%TNFα+
%IFNγ+TNFα+
Anti-CD3
Anti-CD3+Antioxidant
c
MitoQ
MitoTempo
Fold increase MTQ treated / untreated
Fold increase MTT treated / untreated
p=0.0193
Chr
Res
IFN γ+
TNF α+